

Eutectoid Magnetite in Wüstite Under Conditions of Compressive Stress and Cooling

C. H. Zhou · H. T. Ma · Y. Li · L. Wang

Received: 13 October 2010/Revised: 31 October 2011/Published online: 11 May 2012
© Springer Science+Business Media, LLC 2012

Abstract During hot rolling, the existence of a wüstite layer is favored from the standpoint of improved descaling performance. In this work, the mutual effect of external compressive stress and cooling on the phase transformation of oxide scales formed on steel was investigated. Optical microscopy images showed that a fast cooling rate of about 80 °C/min promoted the formation of magnetite/Fe eutectoid. When applying a compressive stress, growth of the magnetite/Fe eutectoid was increased. It was inferred that the promoting effect of fast cooling rate on the diffusion is advantageous to the growth of magnetite/Fe eutectoid. The increase of system chemical potential by the compressive stress also promoted the growth of magnetite/Fe eutectoid.

Keywords Steel · Oxidation · Compressive stress · Magnetite · Wüstite · Cooling

Introduction

The oxide scales formed on a steel affects the friction and thermal conductivity between the roll and the steel interface, which will result in changes in rolling parameters, surface quality and even the properties of the steel [1, 2]. Thus the

C. H. Zhou (✉) · H. T. Ma · L. Wang
School of Materials Science and Engineering, Dalian University of Technology,
Dalian 116085, China
e-mail: dlut2325@163.com

C. H. Zhou
Postdoctoral Research State of Materials Science and Engineering, Harbin Institute of Technology,
Harbin 150001, China

C. H. Zhou · Y. Li
Center for Composite Materials and Structure, Harbin Institute of Technology, Harbin 150001,
China

characteristics of oxide scales are a major concern in the design of rolling technology.

During hot rolling, the scale formed is plastic and can be elongated with the strip because the temperature is higher than 800 °C [3, 4]. After finishing mill, the strip is cooled by water spray to temperatures between 500 and 720 °C. During the cooling process, the scales on the strip surface continue to grow, and usually a three-layer scale consisting of a thinner outermost hematite, a thin intermediate magnetite and a thick inner wüstite layer forms above 570 °C [5]. As wüstite is unstable below 570 °C [6], the oxide-scale microstructure changes according to the cooling rate and the start cooling temperature. Wüstite decomposition induces proeutectoid magnetite precipitation within the wüstite, and even a magnetite seam forming at the scale/steel interface [7–9].

The descaling performance during hot rolling is significantly affected by the oxide-scale microstructure [7]. It is well known that wüstite is easier to remove by the pickling process than magnetite [7], and many previous studies have focused on this aspect. In those studies, a C-curve was often quoted to define the cooling rate to avoid formation of the magnetite layer, especially at the scale/steel interface [10]. However, the actual mechanism for the formation of this layer is still in dispute and a quantitative understanding of the relationship between the cooling conditions and the formation of this layer is still lacking. In addition, stresses in the scale during rolling and coiling are inevitable. According to the literature, applying a stress can change the oxide products [11] and induce changes in the oxide-scale integrity [12], internal oxidation [13], oxidation kinetics [14–16], etc. Thus, the effect of inevitable stress on the oxide-scale microstructural changes should be comprehensively considered in regard to the descaling performance, giving some information on the relationship between the cooling conditions and the oxide-scale microstructure. In the present work, the evolution of oxide-scale microstructure formed on a steel under the conditions of compressive stress and cooling was investigated. The aim was to explore the mutual effect of external compressive stress and cooling on the decomposition of wüstite.

Experimental Procedures

The testing material was a mild-steel plate and its composition was 0.01 wt% C, 0.15 wt% Mn, 0.05 wt% Si, 0.02 wt% Ni, 0.01 wt% Cr, other trace elements 0.04 wt%, and Fe balance. The coupons with dimensions of 6 × 6 × 10 mm for compressive test and 2 × 6 × 10 mm for comparing test without stress were ground with SiC papers down to a 2,000 grit finish (2.5 μm). Prior to oxidation, the coupons were cleaned with acetone and ethanol. After drying, the specimens were subjected to oxidation testing.

Oxidation tests were carried out in air at 700 °C. A high-temperature creep furnace was used to carry out the tests. The compressive samples were subjected to stresses of 5, 10, 15 MPa. The temperature evolution versus time during cooling is represented in Fig. 1. The air-cooled samples reached 200 °C (wüstite transformation does not occur lower than 200 °C [8]) after 6 min from 700 °C, while the

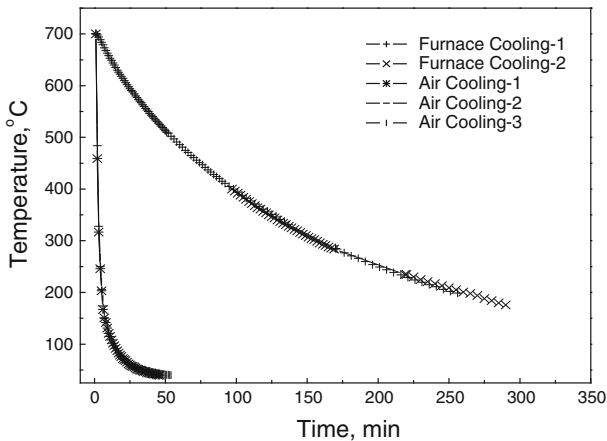


Fig. 1 Continuous cooling curves from the temperature of 700 °C

furnace-cooling samples reached 200 °C after approximately 250 min. The cooling rate during air-cooling was about 80 °C/min and it was approximately 2 °C/min for the furnace-cooling case by calculating. For the compressive test, the samples were loaded into the furnace when the temperature reached the set value, kept there for 10 min, then cooled by either air cooling or furnace cooling. At the same time the compressive stress was applied. The direction of stress was perpendicular to the growth of oxide scales, as shown in the optical microscopy (OM) images.

After the continuous cooling tests, the samples were mounted in resin and cross-sections of the oxide-scale microstructure were prepared using standard metallographic methods. All oxidized samples were revealed using an etchant containing 1 % HCl in ethanol [7, 9]. The etchant attacked both the hematite and wüstite phases, but essentially left the magnetite and the steel substrate unetched. The scale structures were examined using OM.

Results and Discussion

Evolutions of the oxide-scale microstructures for the samples oxidized during continuous air cooling from 700 °C to room temperature are shown in Fig. 2. Figure 2a indicates that the oxide scales on the samples without stress were consisted of an outer magnetite, an inner wüstite, numerous magnetite precipitates within the wüstite layer and mainly near the magnetite layer. When subjecting stresses to the samples, however, the wüstite layer was found to transform into a mixture of magnetite layer, mostly magnetite/iron eutectoid layer, and very often a small amount of retained wüstite, as shown in Fig. 2b, c. Compared with the unstressed condition, apparent growth of the magnetite layer and formation of the magnetite/iron eutectoid layer in wüstite layer were observed in the case of 5 MPa, as displayed in Fig. 2b. Up to 15 MPa, the amount of retained wüstite was so few that no continued layer of wüstite was existed, as indicated in Fig. 2c.

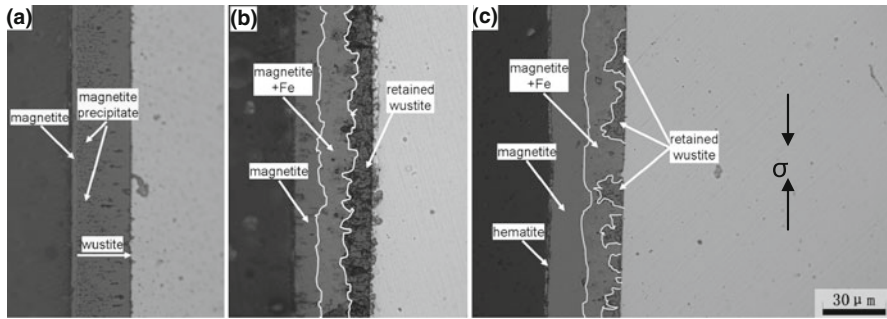


Fig. 2 Oxide scale structures developed under a stress of **a** 0 MPa; **b** 5 MPa; **c** 15 MPa during air cooling at start cooling temperature of 700 °C ($\rightarrow\sigma\leftarrow$ shows the direction of stress)

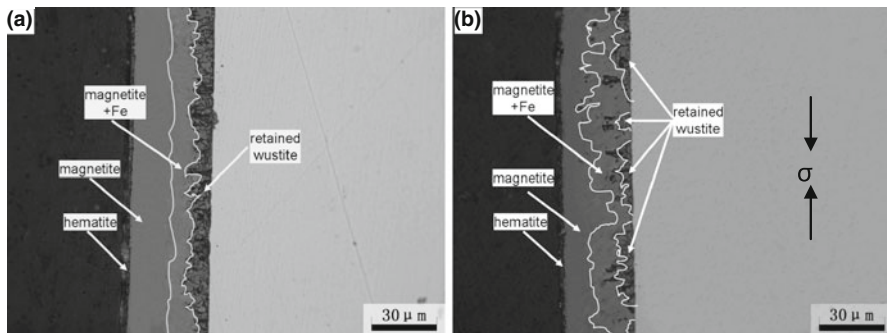


Fig. 3 Oxide-scale structures developed under a stress of **a** 0 MPa; **b** 10 MPa during furnace cooling at start cooling temperature of 700 °C ($\rightarrow\sigma\leftarrow$ shows the direction of stress)

In the case of furnace cooling, oxide scales on the samples without stress were composed of an outer thinner hematite layer, a thicker magnetite layer, a magnetite/wüstite eutectoid layer and a continued retained wüstite layer, as shown in Fig. 3a. However, Fig. 3b shows that the formed oxide scales subjected to 10 MPa stress comprised less discontinuous retained wüstite.

A structural study of oxide scales formed on the hot-rolled steel strip by simulated coiling and cooling was performed by Chen [7], who defined the oxide-scale microstructure as three types. Type I means that some magnetite precipitates forms inside the wüstite layer. Type II is designed as more magnetite precipitates generates inside the wüstite layer and magnetite seam appears at the scale/steel interface. For the Type III, the wüstite layer in the scale is transformed into a mixture of mostly magnetite/iron eutectoid, a certain amount of precipitated magnetite and very often a small amount of retained wüstite. In the view of applying stress, the evolution of oxide-scale microstructure is as follows:

Air cooling: Type I (0 MPa) \rightarrow Type II (5 MPa) \rightarrow Type III (15 MPa)

Furnace cooling: Type II (0 MPa) \rightarrow Type III (10 MPa)

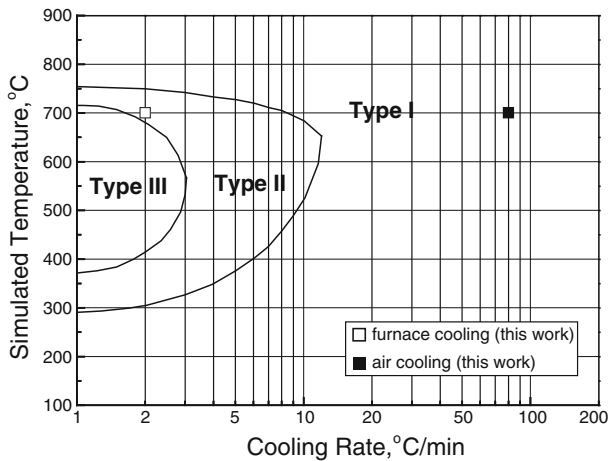


Fig. 4 Scale type versus simulated coiling temperature and strip-cooling rate [7, 8]

A C-curve was proposed by Chen [7, 8], which shows oxide-scale type versus simulated temperature and cooling rate, as given in Fig. 4. Seen from Fig. 4, it can be gained that the oxide-scale microstructures for air cooling and furnace cooling without stress should belong to Type I and Type II, respectively. These are consistent with the Figs. 2a and 3a. Different oxide-scale microstructures would form under different cooling conditions, such as cooling rate, start cooling temperature. Then oxide-scale microstructural changes are related to the wüstite decomposition. Large numbers of literatures have been concerned on the isothermal decomposition [17–19]. The decomposition of wüstite during cooling, however, is studied sparsely. Nonetheless, it is indicated that the oxide-scale microstructure will change in a wide range at different cooling rates under continuous cooling conditions [7–9]. The observations of the samples without stress are in agreement with the published results, i.e., fast cooling rate induces the formation of magnetite precipitates in wüstite layer.

The disproportionation of isothermal condition generally takes place in three stages [20]: I. pre-precipitation; II. formation of magnetite with a corresponding enrichment in iron for the remaining wüstite; and III. formation of metallic iron and more magnetite. According to the C-curve relationship of isothermal decomposition of wüstite [10], as shown in Fig. 5, the cooling rate is about 75 °C/min for the initial formation of magnetite layer. Therefore, no visible magnetite layer formed in the case of air cooling because its cooling rate of 100 °C/min is higher than the aforementioned estimated rate. It is attributed to that Fe ion diffusion is restricted at such a fast cooling rate, and some chain-like precipitations are formed, as shown in Fig. 2a. Those processes are similar to the stage I of isothermal disproportionation. While in the case of 2 °C/min, there is enough time for Fe ions diffusion and thereby wüstite transforms to magnetite/Fe eutectoid. These processes maybe undergo stage II, III, or both. Although it is not examined here, the final results in Fig. 3a are in agreement with the previous results [7, 9, 10].

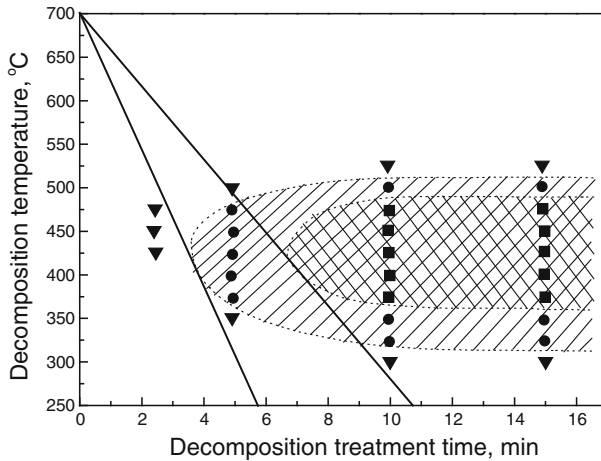


Fig. 5 Isothermal formation of a magnetite layer at the wüstite-steel interface: *black square* continuous magnetite (Fe_3O_4) layer, *black circle* Fe_3O_4 nucleation, and *inverted triangle* no visible Fe_3O_4 was observed [10]

A viewpoint of chemical potential is considered to analyze the effect of applying compressive stress on the decomposition of wüstite. It is known that the external stress would induce a change in system chemical potential. The change of chemical potential owing to the external stress is called as mechanical–chemical potential, and it can be calculated as the following equation [21].

$$\Delta u = \int_{p_1}^{p_2} V(p) dp \quad (1)$$

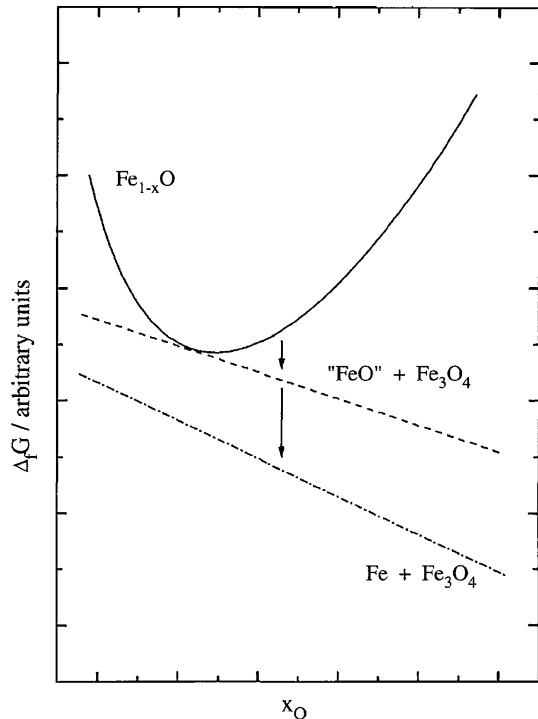
Further:

$$u = u_{\Delta p=0} + V_0 \Delta p \quad (2)$$

where u is mechanical–chemical potential, $u_{\Delta p=0}$ chemical potential, V_0 molar volume of scale, Δp residual compressive stress. Then, it can be easily gained that applying a compressive stress increases the driving force of decomposition from wüstite to magnetite/iron eutectoid. The more compressive stress is applied, the more amount of magnetite/Fe eutectoid is formed, just like the showing in Fig. 2. In addition, according to the diagram of Gibbs energy showed in Fig. 6 [22], a two-phase metastable intermediate product of FeO and Fe_3O_4 is initially formed, which results in the subsequent occurrence of an iron-rich wüstite simultaneously with the exsolution of magnetite. When a stress is applied, the increased Gibbs energy by the applying compressive stress promotes the intermediate product formation and even leads to the final formation of magnetite/Fe eutectoid at a fast cooling rate.

Moreover, the effect of compressive stress on the oxide-scale integrity needs to be considered. An applying compressive stress can induce more pores or even cracks form in or near surface of the oxide scales [23–26], thereby the inward

Fig. 6 Schematic diagram of the Gibbs energy of formation for the relevant phases in the Fe–O system [21]



transportation of oxygen and outward diffusion of metallic ions along such short circuits can be promoted. Then, the oxide scales would grow fast, and the magnetite grows as the equation: $6\text{FeO} + \text{O}_2 \rightarrow 2\text{Fe}_3\text{O}_4$ or $3\text{FeO} + \text{O}^{2-} \rightarrow \text{Fe}_3\text{O}_4 + 2\text{e}^-$. Accordingly, the retained wüstite is decreased owing to the growth of magnetite and the eutectoid of magnetite/Fe in wüstite layer.

Conclusions

This work investigated the mutual effect of compressive stress and cooling conditions on the morphological development of oxide scale on pure Fe, emphasizing on the microstructural evolution of the wüstite layer. The results indicated that:

- (1) Applying a compressive stress resulted in the decomposition of wüstite and the formation of magnetite/iron eutectoid in the initial wüstite layer. The amount of retained wüstite decreased with the increasing stress.
- (2) Growth of the magnetite/Fe eutectoid, i.e., wüstite decomposition, was promoted by higher cooling rate.

References

1. P. A. Munther and J. G. Lenard, *Journal of Materials and Processing Technology* **88**, 105 (1999).
2. M. Torresa and R. Colas, *Journal of Materials and Processing Technology* **105**, 258 (2000).
3. W. L. Roberts, *Hot Rolling of Steel*, (Marcel Dekker, New York, 1983).

4. R. M. Guo and J. J. M. Too, *Recent Advances in Heat Transfer and Micro-Structure Modelling for Metal Processing*, (ASME, Metals Park, 1995).
5. W. Gao and Z. W. Li, *Developments in High-Temperature Corrosion and Protection of Materials*, (Woodhead Publishing Ltd, Cambridge, 2008).
6. T. B. Massalski, H. Okamoto, and P. R. Subramanian, *Binary Alloy Phase Diagrams*, (ASME, Metals Park, 1990).
7. R. Y. Chen and W. Y. D. Yuen, *Oxidation of Metals* **53**, 539 (2000).
8. R. Y. Chen and W. Y. D. Yuen, *Oxidation of Metals* **59**, 433 (2003).
9. R. Y. Chen and W. Y. D. Yuen, *Oxidation of Metals* **57**, 53 (2002).
10. J. Baud, A. Ferrier, and J. Manenc, *Oxidation of Metals* **12**, 1978 (331).
11. R. Rolls and M. H. Shahhosseini, *Oxidation of Metals* **18**, 115 (1982).
12. J. Robertson and M. I. Manning, *Materials Science and Technology* **6**, 81 (1990).
13. G. Calvarin-Amiri, R. Molins, and A. M. Huntz, *Oxidation of Metals* **53**, 399 (2000).
14. C. H. Zhou, H. T. Ma, and L. Wang, *Corrosion Engineering, Science and Technology* **44**, 358 (2009).
15. C. H. Zhou, H. T. Ma, and L. Wang, *Corrosion Science* **52**, 210 (2010).
16. C. H. Zhou, H. T. Ma, and L. Wang, *Oxidation of Metals* **71**, 335 (2009).
17. B. Ilschner, *Acta Metallurgica* **13**, 855 (1965).
18. J. Paidassi, *Acta Metallurgica* **3**, 447 (1955).
19. L. Broussard, *Journal of Physical Chemistry* **73**, 1848 (1969).
20. B. Gleeson, S. M. M. Hadavi, and D. J. Young, *Materials at High Temperatures* **17**, 311 (2000).
21. М. Гутманъ, *Mechano-Chemistry of Metals and Protection from Corrosion* (trans by S. Jin), (Science Press, Beijing, 1989).
22. Svein Stølen, Ronny Glöckner, and Fredrik Grønvold, *Thermochimica Acta* **256**, 91 (1995).
23. C. H. Zhou, H. T. Ma, and L. Wang, *Journal of Dalian University of Technology* **50**, 667 (2010).
24. R. Bhattacharya, G. Jha, S. Kundu, R. Shankar and N. Gope, *Surface and Coatings Technology* **201**, 526 (2006).
25. Y. Ikeda and K. Nii, *Oxidation of Metals* **12**, 487 (1978).
26. W. Christl, A. Rahmel and M. Schütze, *Oxidation of Metals* **31**, 1 (1989).